# Removal of Copper Ions from Aqueous Solutions via Adsorption on Carbon Nanocomposites

Anthony B. Dichiara, Michael R. Webber, William R. Gorman, and Reginald E. Rogers*

Department of Chemical Engineering, Rochester Institute of Technology, Rochester, New York 14623, United States

ABSTRACT: The development of technologies for water purification is critical to meet the global challenges of insufficient water supply and inadequate sanitation. Among all wastewater treatments, adsorption is globally recognized as the most promising method because of its versatility and economic feasibility. Herein, the removal of copper ions (Cu(II)) from aqueous solutions through adsorption on free-standing hybrid papers comprised of a mixture between graphene and different types of carbon nanotubes (CNTs) was examined. Results indicate that the rate of adsorption and long-time capacity of the metal ions on the nanocomposites significantly exceeds that of activated carbon by a factor of 4.

Moreover, the combination of graphene with CNTs endows an increase in the uptake of Cu(II) up to 50% compared to that of CNTs alone, with a maximum adsorption capacity higher than 250 mg·g^{-1}. The removal of Cu(II) from water is sensitive to solution pH, and the presence of oxygen functional groups on the adsorbent surface promotes higher adsorption rates and capacities than pristine materials. These hybrid nanostructures show great promise for environmental remediation efforts, wastewater treatments, and separation applications, and the results presented in this study have important implications for understanding the interactions of carbonaceous materials at environmental interfaces.

KEYWORDS: adsorption, graphene, carbon nanotube, composite, wastewater treatment, metal ions
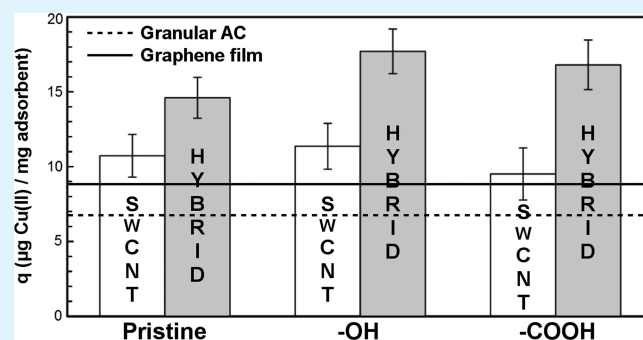
1. INTRODUCTION

The availability of freshwater that is free from toxic chemicals and pathogens, is an important issue for agriculture, industry and human health.[1] In particular, the contamination of aqueous systems by toxic heavy metals like copper poses serious threats to the environment, especially in developing countries with less stringent regulations. Although most metals are essential nutrients at a trace level, they are nonbiodegradable and can accumulate in living organisms where they can be harmful at high concentrations.[2] The ingestion of copper for long periods of time at levels above the regulation limit (i.e., 1.3 mg/L, established by the U.S. Environmental Protection Agency) has deleterious effects on human health, potentially causing depression and severe irritation of the gastrointestinal and nervous systems.[3] Copper pollution is a serious and rising environmental concern because of the possibility of dissolved ions leaching from plumbing materials after corrosion of domestic and commercial water distribution systems.[4] The contamination of copper in hydrological environments can also be the result of erosion of natural deposits, industrial discharge, and road runoff because of the release of copper from automobiles.[5] Therefore, the removal of concentrated copper from aqueous solutions is of paramount importance.

In recent years, carbon nanomaterials like nanotubes (CNTs) or graphene have been increasingly studied as attractive adsorbents for wastewater treatments because of their unique properties.[6,7] Capitalizing on their open pore structure, high surface area, large delocalized π electrons, and hydrophobic surface, graphene and CNTs exhibit better or at least comparable adsorption capacities than activated carbon (AC), which is to date the world's most widely used adsorbent.[8−10] A recent study revealed that the optimum carbonaceous nanoparticle design to enhance copper adsorption did not match any currently available materials.[4] The development of hierarchical assemblages by the combination of graphene and CNTs into nanohybrid materials offers an efficient way of engineering novel nanostructures with superior adsorption attributes.[11] Such conjugations between CNTs and graphene provide higher exfoliation degrees along with the formation of an open and hierarchical pore structure, hence increasing the number of available sites for adsorption.[12] However, there have been relatively few studies that have explored the potential of these types of carbonaceous nanocomposites in water purification systems. Prior investigations have reported enhanced adsorption of polyaromatic compounds[13] and pesticides[14] on CNT−graphene hybrids compared to each component alone. This further motivates the examination of such nanocomposites for the removal of copper ions, Cu(II), from hydrological environments.

The present study describes the aqueous-phase adsorption of Cu(II) on free-standing hybrid papers comprised of both graphene and single-wall CNTs (SWCNTs). Different types of SWCNTs are considered: pristine and OH- and COOH-functionalized SWCNTs. The adsorption of Cu(II) on commercially available activated carbon (AC) is also reported for comparison purposes. The influence of experimental conditions such as contact time or solution pH is studied to provide an understanding of the adsorption mechanism. Results demonstrate the great potential of carbon-based nano-composites for versatile water purification and treatment.

2. EXPERIMENTAL SECTION

2.1. Materials and Chemicals. Granular activated carbon (AC) was purchased from Calgon Carbon Corp. (Filtrasorb 100) and used as-received without further treatment. Pristine and functionalized (−OH and −COOH) single-wall carbon nanotubes (SWCNTs) were obtained from Cheap Tubes, Inc. The CNT length is below 30 μm, the individual tube inner diameter ranges between 0.8 and 1.6 nm, and the purity is higher than 90%. Graphene nanoplatelets were purchased from Angstron Materials (N002-PDR). The size of the graphene flakes is approximately 10 μm, with thickness lower than 1 nm and purity higher than 95%. N,N-Dimethylacetamide with 99% purity was obtained from Sigma-Aldrich. Copper nitrate hemi(pentahydrate) with 98% purity was used for Cu(II) adsorption, and it was purchased from Alpha Aesar. All materials and chemicals were used as-received without any further treatment, and ultrapure water was obtained from a Milli-Q water filtration station (18.2 MΩ·cm at 20 °C).

2.2. Sample Preparation. Free-standing graphene−CNT hybrid papers were prepared using a vacuum-assisted filtration procedure as previously reported.[12] Briefly, each type of SWCNTs (pristine, −OH, and −COOH) was dispersed with graphene nanoplatelets in N.N-dimethylacetamide by ultrasonication for 45 min. The temperature of the sonication bath was kept at 25 °C by changing the water every 20 min to avoid over heating. The mass ratio of SWCNT to graphene was set to 2:1 because it showed larger uptakes for a large variety of compounds.[12] The resulting solutions were then passed through a 47 mm, 0.2 μm pore size PTFE membrane (Pall Corporation, USA) supported on a fritted glass holder that was first wetted with methanol (BDH, 99%) to allow easy release of the carbonaceous films from the membrane filters through the volatilization of methanol. No binder was used at any stage. The films were peeled from the membranes and dried at 60 °C for 1 h without rinsing to avoid reaggregation. The resulting free-standing papers were cut into smaller sections (0.5 cm^2) and weighed on an ultramicrobalance (Mettler-Toledo, XS204) with each section weighing 0.6 ± 0.05 mg. The as-prepared papers were further dried at 110 °C for 48 h to remove moisture and to overcome the competitive Coulombic stability of the deprotonated carboxylic acid by the polar water molecules and ammonium cations during adsorption analysis.

2.3. Characterization. The morphology of all samples was characterized prior to adsorption using a field emission scanning electron microscope (FE-SEM, Hitachi S-900) operated at 2 kV, whereas the surface functional groups were analyzed in air by Fourier transformed infrared spectroscopy (FTIR, Shimatzu IR Prestige-21). For the FTIR measurements, the spectra of the pristine nano-composite served as the background for the analysis of the other samples. Raman spectra of all specimens were acquired from a JY-Horiba Labram spectrophotometer equipped with a 632.6 nm He/Ne laser as the excitation radiation. Optical contact angle measurements were obtained using a Rame-Hart 250 goniometer. Ultrapure water was dispensed in the form of drops through a microsyringe. The contact angle was evaluated by using the tangent method and averaged over ten measurements for each sample.

2.4. Adsorption Studies. Artificial wastewater was prepared by spiking ultrapure water with doses of copper nitrate hemi-(pentahydrate), resulting in solutions of Cu(II) at environmentally relevant concentrations, which are typically in the microgram per milliliter range (i.e., 5−30 μg/mL).[4,5] The solution pH was measured by a pH meter (Mettler Toledo FG2) and was adjusted using 1 M HCl or 1 M NaOH to the range of 3.7−6.8. The predominant copper species in this pH range are Cu(II). Unless otherwise specified, the solution pH was set to 6.8. UV/vis absorption spectroscopy (PerkinElmer Lambda 950 UV/vis/NIR) was conducted to determine the solution concentrations using a measured extinction coefficient from Beer's law analysis. The amount of copper adsorbed per mass of adsorbent, q, was deduced by subtracting the mass of adsorbate in solution at a given time from the initial mass of adsorbate in solution. Both short-time and isotherm adsorptions were studied at 20 °C in a batch adsorption vessel (10 mL) placed on an orbital shaker platform operated at 120 rpm (Bel-Art Spindrive). Equilibrium was declared when there was no appreciable change in solution concentration with additional contact time. Blank adsorption experiments were performed without any adsorbent to ensure that no molecule was adsorbed on the wall of the container. For statistical soundness, data presented henceforth correspond to the average among triplicate trials, with typical errors being less than 8%.

3. RESULTS AND DISCUSSION

3.1. Adsorbents Characterization. In practical applica-tions, the choice of adsorbent is not only based on its intrinsic properties, such as selectivity, capacity, mass transfer rate, and long-term stability, but also includes economical considerations. Whereas granular AC is still more affordable than nanotubes or graphene, the latter can be used as free-standing papers, which can balance their relatively high cost. As opposed to powder-like materials (inset Figure 1a), the as-prepared free-standing
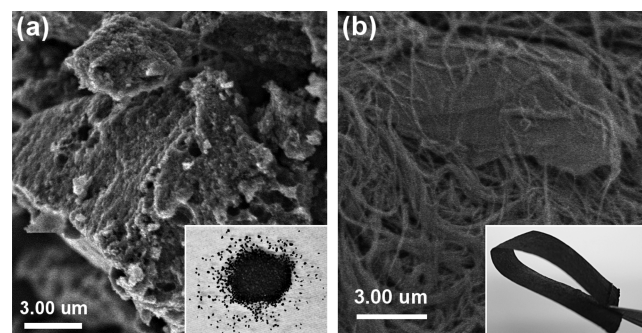

Figure 1. SEM images of (a) granular activated carbon and (b) as-prepared SWCNT−graphene hybrid. Their respective digital photo-graphs are shown in the insets.

hybrid adsorbents do not require any additional procedure for solid−liquid separation, such as filtration, centrifugation, or flocculation.[15] The carbonaceous free-standing membranes are extremely flexible (inset Figure 1b) and exhibit impressive mechanical strength.[16,17] The thickness of the free-standing papers ranges from 10 to 30 μm as measured by cross-sectional electron microscopy. They also present a very high stability in aqueous solutions, and no significant deteriorations or mass losses have been observed under a wide range of conditions (i.e., solution pH, agitation speed, and temperatures).

As revealed by scanning electron microscopy, the different carbonaceous materials show very distinct morphological features. Granular AC has a very rough structure characterized by irregular edges, cracks and cavities (Figure 1a), whereas graphene and SWCNT have a rather smooth surface (Figure 1b). In Figure 1b, it can be seen that the SWCNTs are able to closely contact the graphene flakes because of their strong $\pi-\pi$ interactions,[18] forming a hierarchical network with an open pore structure. The graphene nanoplatelets are found to be

evenly distributed into the SWCNT matrix, and in most cases, they orient themselves parallel to the plane of the paper. Similar morphological features without any distinctive differences are observed for all types of nanocomposites, including both pristine and oxidized materials.

Contact angle measurements were conducted on the pristine and oxidized nanocomposites, and the results are shown in Figure 2. The pristine SWCNT−graphene hybrid exhibits a
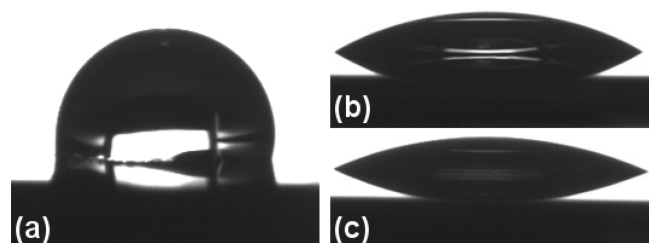

Figure 2. Images of water drops forming a contact angle of 103.8, 32.1, and 23.7° on the surface of (a) pristine and (b) COOH- and (c) OH-functionalized nanocomposites, respectively.

very low wetting surface with a contact angle of 103.8° (Figure 2a). However, the contact angle values of the oxidized materials are much lower, which can be associated with the higher number of polar groups on their surface, thus endowing a hydrophilic behavior (Figure 2b,c). These observations are consistent with previous studies reporting the effect of surface oxidation on the wettability of carbon nanostructures.[19]

Typical Raman spectra of the different nanocomposites are presented in Figure 3a. All carbonaceous materials display strong peaks near 1336 and 1590 cm^{-1}, assigned to the D band and G band, respectively. The G band is the characteristic peak for the stretching vibration of carbon sp^2 bonds in a hexagonal lattice, whereas the D band is the characteristic peak for the vibration of carbon atoms with dangling bonds in an amorphous carbon network.[20] The integrated intensity ratios of the D band to the G band (I_D/I_G) reflect the degree of graphitization of the carbon surfaces for each type of adsorbent.[21] The pristine SWCNT−graphene structure presents the highest structural integrity as indicated by the lowest I_D/I_G value (i.e., 0.2). The OH- and COOH-functionalized nanocomposites show higher I_D/I_G values of 0.9 and 0.8, respectively. It is commonly held that typical oxidation

procedures used to increase the amount of functional groups on carbon nanomaterials also induce unavoidable damages to the graphitic structure.[22] Among all adsorbents, granular AC has the highest ratio of I_D/I_G (i.e., 1.1). Hence, both pristine and oxidized hybrid materials appear to be composed of more completely crystallized sp^2-bonding graphitic surfaces than granular AC.

The major functional groups of the different carbonaceous materials were identified by FTIR spectroscopy. The FTIR spectra of OH- and COOH-functionalized hybrids and AC are presented in Figure 3b. All FTIR spectra of carbonaceous materials exhibit absorption peaks located around 1392 cm^{-1}, which can be attributed to the disordered structure of graphite.[23] The presence of peaks around 2860 and 2924 cm^{-1} are also observed because of the asymmetric/symmetric stretching of ethylene groups that are usually located at defect sites.[24] Moreover, the IR spectra of the oxidized adsorbents show other major peaks located around 1560, 1738, 2362, and 3726 cm^{-1}.[25] The peak at 1560 cm^{-1} is related to the carboxylate anion stretch mode, whereas the feature at 1738 cm^{-1} is associated with the stretch mode of carboxylic groups. Finally, the peak at 2362 cm^{-1} corresponds to the O−H stretch from strongly hydrogen-bonded −COOH, and the peak at 3726 cm^{-1} is assigned to free hydroxyl groups.

3.2. Short-Time Adsorption. The short-time adsorption of Cu(II) on the different carbonaceous materials is shown in Figure 4a. The removal of Cu(II) from water increases linearly for all adsorbents over the entire 3 h time period. The most striking observation is that the adsorption of Cu(II) is significantly higher on the nanocomposites than on AC and that the rate of adsorption is faster. Moreover, the uptake of Cu(II) on the functionalized nanocomposites is higher than on the other adsorbents over the entire 3 h time period. The retention of copper ions increases in the order of OH-functionalized hybrid > COOH-functionalized hybrid > pristine hybrid > granular AC.

By comparing Figure 2 with Figure 4, it can be seen that the adsorption of Cu(II) on the surface of carbon-based materials is inversely correlated with the contact angle between water and the adsorbent surface. These observations show that the presence of oxygen functional groups plays a key role in the interactions between Cu(II) and carbonaceous surfaces. Pristine carbonaceous materials (i.e., AC and pristine hybrid)
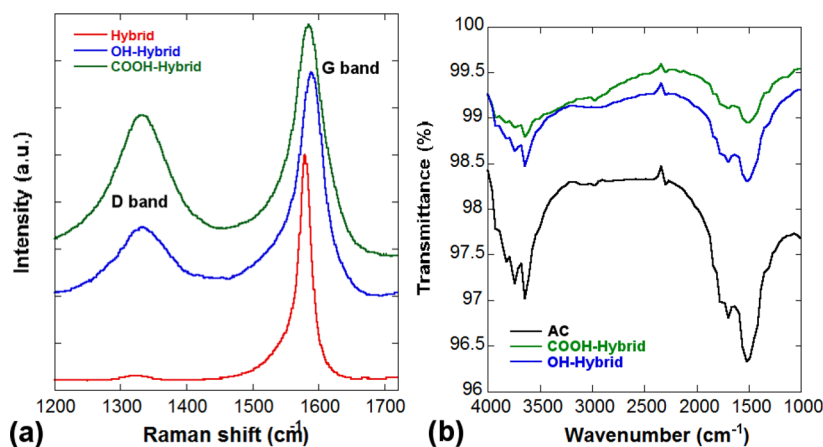

Figure 3. (a) Raman spectra of as-prepared pristine and OH- and COOH-functionalized hybrids prior to adsorption studies. (b) FTIR spectra of OH- and COOH-functionalized hybrids and as-received activated carbon (AC).
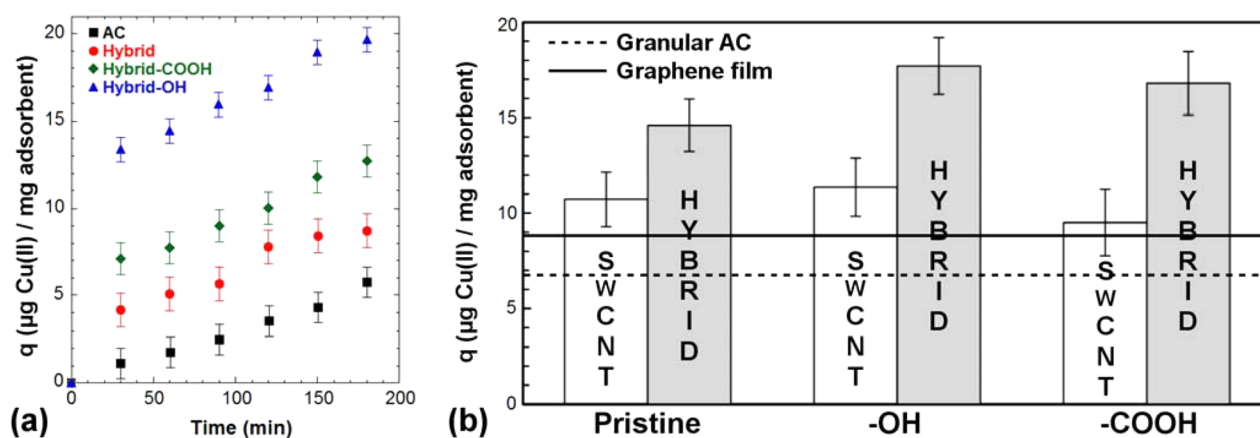
Figure 4. (a) Time-dependent adsorption of Cu(II) on different carbonaceous materials for a 3 h time period (temperature: 20 °C; initial concentration: 25 $\mu g \cdot mL^{-1}$; solution pH 6.8). (b) Uptakes of Cu(II) on pristine and COOH- and OH-functionalized SWCNTs and their hybrid counterparts. The straight and the dashed lines correspond to the uptake of Cu(II) on graphene and granular AC, respectively (temperature: 20 °C; initial concentration: 20 $\mu g \cdot mL^{-1}$; solution pH 6.8).

have very few oxygen groups on their surface (Figure 3b) and consequently afforded lower Cu(II) uptakes. Despite the fact that carboxyl functional groups have been found to induce a larger and more consistent increase in Cu binding energies,[26] the OH-functionalized nanocomposite exhibits much larger Cu(II) retentions over the 3 h time period than those of the COOH-functionalized nanocomposite. The COOH- and OH-functionalized hybrids contain 2.7% COOH groups and 3.9% OH groups, respectively (given by the manufacturer), suggesting that the adsorption is positively correlated with the concentration of oxygen groups. This is consistent with other studies reporting the adsorption of metal ions on carbonaceous materials.[4,8−10] Previous theoretical calculations demonstrated that the chemically active oxygen in the functionalized CNT surfaces can enhance the binding of Cu with carbon nanomaterials by promoting the electron exchange between Cu and carbon atoms or directly interacting with Cu.[26] Such reactions between the divalent metal cations with the oxidized nanostructures can lead to the release of H⁺ ions into the water, slightly decreasing the solution pH, which was observed in some experiments.[27]

Besides the presence of oxygen functional groups, recent studies revealed that the intrinsic wrinkles on graphene nanosheets can induce inhomogeneities in the charge distribution so that concentrated charges are located at the wrinkles, thus resulting in more energetically favorable regions for the adsorption of diverse molecules.[28] The presence of these wrinkles may also contribute to the sieving effect by forming powerful groove regions on the graphene surfaces.[29] The sieving effect can also play an important role in Cu(II) decontamination because the accessibility of adsorption regions for metal ions is expected to be quite different for the nanocomposites than AC. The hybrid nanomaterials exhibit an open pore network that facilitates fast molecular diffusion and promotes the accessibility of adsorption sites (Figure 1b), as opposed to the closed, irregular-shaped micropore structure of granular AC (Figure 1a).

Figure 4b provides a comparison between the adsorption of Cu(II) onto different types of SWCNTs and their hybrid counterparts after 24 h under constant agitation. It can be observed that in each case the uptake of Cu(II) per unit mass of adsorbent is always higher when the SWCNTs are combined with graphene promoting an improvement in adsorption

capacities on the order of 50% better than that of the SWCNTs alone. This is consistent with our previous work about the adsorption of various organic compounds on similar carbon-based nanocomposites.[12] The effective intercalation and distribution of CNTs in between the graphene sheets, the higher degree of exfoliation of graphene in the presence of CNTs, and the formation of a porous architecture between these carbon nanostructures are expected to endow the nanocomposites with a larger amount of sites available for adsorption. As a result, the specific surface area of such kinds of hybrid materials is in general higher than each component alone.[30]

3.3. Effect of Solution pH. The solution pH is one of the most important parameter controlling the adsorption of metal ions on the surface of carbonaceous materials because it influences both the surface chemical properties of the adsorbent and the solution chemistry of the adsorbate in aqueous solution. The effect of solution pH is illustrated in Figure 5. It can be observed that Cu(II) adsorption occurs under acidic pH conditions. The uptake of Cu(II) increases with the increase in pH for all adsorbents, reaching maximum uptake values at 6.8. Within the pH range studied (i.e., from 3.7 to 6.8), the removal
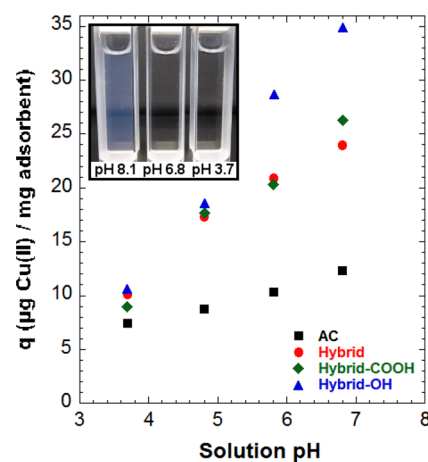

Figure 5. Effect of solution pH on the adsorption of Cu(II) on the surface of carbonaceous adsorbent (temperature: 20 °C; initial concentration: 25 $\mu g \cdot mL^{-1}$).
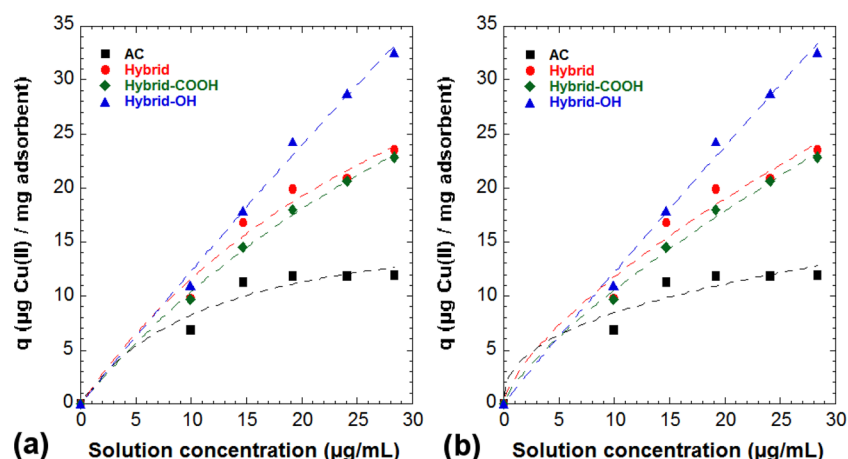
Figure 6. Adsorption isotherms of Cu(II) on different carbonaceous materials at 20 °C. The curve fits (dashed lines) correspond to (a) Langmuir and (b) Freundlich isotherms.

of Cu(II) is solely due to adsorption because no precipitation was detected at the given initial concentration. However, the hydroxide precipitation of Cu(II) is observed at alkaline pH, as depicted in the inset in Figure 5. These results are consistent with previous studies reporting the adsorption of metal cations on various carbonaceous adsorbents.[31−33]

At low solution pH, the functional groups on the oxidized adsorbent surface (i.e., hybrid−OH and hybrid−COOH) are protonated, forming a positive surface charge.[33] Similar reactions occur on the surface of pristine carbonaceous materials (i.e., AC and hybrid); a bond may be established between H_3O^+ ions and the cloud of π electrons of the aromatic rings of graphitic carbon. This induces the electrostatic repulsion between the positively charged adsorbent surface and the free cations in aqueous solution. In addition, there is a competition between H^+ and Cu(II) ions for the limited active sites.[34] These two phenomena lead to low adsorption rate at pH <4. Although Cu(II) adsorption takes place under acidic conditions, higher acidic pH (i.e., pH >4) promotes the ionization of the oxygen-containing functional groups on the surface of the adsorbents that play a significant role in the uptake of Cu(II). Moreover, when the solution pH increases, the concentration of H^+ ions decreases, hence reducing the electrostatic repulsion and the competitive adsorption for higher Cu(II) retention.

Moreover, the adsorption of Cu(II) is more sensitive to solution pH in the case of oxidized adsorbents (i.e., hybrid−OH and hybrid−COOH) than for pristine graphitic materials (i.e., AC and hybrid), as illustrated in Figure 5. This can be explained by the different positions of the point of zero charge (PZC) for each adsorbent. The pH at PZC (pH_{PZC}) defines the Coulombic interactions between the surface of carbonaceous materials and ionic species.[35] Because the surface of carbonaceous adsorbent is positively charged at pH values below pH_{PZC} and negatively charged at pH values above pH_{PZC}, a lower pH_{PZC} induces higher Cu(II) uptake.[36] Previous reports suggested that the presence of surface acidic functional groups on carbonaceous materials, such as −OH or −COOH, decreases the value of pH_{PZC}.[37,38] Therefore, the higher retention of Cu(II) ions on oxidized adsorbents (i.e., hybrid−OH and hybrid−COOH) can be attributed to lower pH_{PZC}.

3.4. Equilibrium Isotherms. For all tested adsorbate/adsorbent combinations, adsorption−desorption equilibrium was reached in less than 24 h under constant agitation. This is

contrasts with previous work reporting the adsorption of Cu(II) on oxidized CNTs.[39,40] In these reports, the Cu(II) adsorption reaches equilibrium in less than 250 min. The difference can be attributed to the higher adsorbent dosages reported in these studies (i.e., 300 mg·L^{-1} as compared with <50 mg·L^{-1} in the present work).

Figure 6 presents equilibrium isotherms at 20 °C for Cu(II) on the different carbonaceous materials. The qualitative behaviors of these isotherms, with a progressive increase in adsorption at lower concentrations, are consistent with reported data for the adsorption of Cu(II) on other types of carbonaceous adsorbents.[8−10] The Langmuir (Figure 6a) and Freundlich (Figure 6b) isothermal models were used to provide a fit to the experimental data. The Langmuir isotherm, corresponding to monolayer sorption on a surface with a finite number of identical sites and uniform adsorption energies, is represented by eq 1, with K_1 and K_2 being the equilibrium constants (mL·mg^{-1}) and C being the concentration of the adsorbate solution (mg·mL^{-1}).[41]

$$q = \frac{K_1 C}{1 + K_2 C} \tag{1}$$

The Freundlich equation, based on phenomena on heterogeneous surfaces, is represented by eq 2, where K_F and n are the Freundlich constants related to the adsorption capacity and adsorption intensity, respectively.[42]

$$q = K_F C^{1/n} \tag{2}$$

Both Langmuir and Freundlich isotherms provide a good fit to the experimental data with correlation coefficient values being close to one. The relative parameters calculated from each isothermal model are listed in Table 1. Granular AC presents the lowest value of K_F extracted from the Freundlich isotherm, hence revealing the minimum Cu(II) uptake capacity

Table 1. Langmuir and Freundlich Parameters

adsorbents	Langmuir			Freundlich		
	K_1	K_2	R^2	K_F	n	R^2
granular AC	1.53	0.09	0.98	1.33	1.04	0.98
pristine hybrid	1.47	0.03	0.98	3.32	2.49	0.98
COOH−hybrid	1.25	0.02	0.99	1.85	1.32	0.99
OH−hybrid	1.28	0.005	0.99	2.44	1.45	0.99

among all carbonaceous adsorbents. This is consistent with the maximum Cu(II) monolayer coverage determined by the ratio between the Langmuir constants K_1 and K_2. The monolayer adsorption of Cu(II) increases in the order of AC > pristine hybrid > COOH−hybrid > OH−hybrid, with maximum values reaching 17, 49, 63, and 256 $\mu g \cdot mg^{-1}$, respectively.

The relative favorability for adsorption can be quantified by the separation factor, R_L defined as[43]

$$R_L = \frac{1}{1 + K_1 C_0} \tag{3}$$

In eq 3, K_1 is one of the equilibrium constants ($mg \cdot mL^{-1}$) from the Langmuir isotherm expressed in eq 1, and C_0 is the initial adsorbate concentration ($mg \cdot mL^{-1}$). The measured Cu(II) adsorption at equilibrium yields R_L values ranging from 0.021 to 0.026, which indicates favorable adsorption on all carbonaceous materials. This is consistent with the adsorption parameter n extracted from the Freundlich isothermal model given by eq 2, which yields values exceeding unity (Table 1). Moreover, the n values are higher for the nanocomposites, thus suggesting stronger bonds with the adsorbate than AC.

Table 2 summarizes the Cu(II) adsorption capacities of different carbonaceous materials. The as-prepared OH-

Table 2. Summary of the Cu(II) Adsorption Capacities of Different Carbonaceous Materials

adsorbents	Cu(II) uptakes (mg/g)	reference
OH−CNT	7	4
COOH−CNT	5.5	4
NaOCl-modified CNT	47	8
oxidized MWCNT	34	9
UV-oxidized SWCNT	250	10
graphene oxide	115	33
oxidized MWCNT sheet	65	44
graphene oxide−CdS	137	45
PVP−graphene oxide	1689	46
granular AC	17	this study
pristine hybrid	49	this study
COOH−hybrid	63	this study
OH−hybrid	256	this study

functionalized nanocomposites exhibit excellent adsorbencies for Cu(II) ions, with a maximum monolayer adsorption significantly larger than the predicted value for the optimum carbonaceous nanoparticle. Although not the highest one ever reported,[46] these uptakes are much higher than those of commercial AC and other recently refined carbonaceous materials, including oxidized nanotubes and graphene oxide.[4,8−10,33,44,45]

4. CONCLUSIONS

Pristine and oxidized SWCNT−graphene nanohybrids have been prepared using a vacuum-assisted filtration procedure without the use of any binder. The obtained nanocomposites are in the form of flexible free-standing papers with a relatively high structural integrity and their wetting behavior depends on the degree of oxygen groups on their surface. All nanocomposites exhibit faster absorption rates and higher uptake capacities for Cu(II) than granular AC. When compared with each component alone (i.e., graphene and SWCNTs), not only the hybrids show better adsorption properties, but they also provide an economical advantage over SWCNTs alone by

reducing the amount of nanotubes per unit mass of adsorbent. The removal of copper ions from water is strongly affected by the solution pH regardless of the nature of the adsorbent. All these features make these carbon-based hybrid nanostructures suitable to clean contaminated aqueous solutions and very compelling for a wide range of applications in water purification and separation treatment.

■ AUTHOR INFORMATION

Corresponding Author
*E-mail: rerche@rit.edu. Tel.: +1 585 475 4157.

Notes
The authors declare no competing financial interest.

■ REFERENCES

(1) Machell, J.; Prior, K.; Allan, R.; Andresen, J. M. The Water Energy Food Nexus − Challenges and Emerging Solutions. *Environ. Sci.: Water Res. Technol.* **2015**, *1*, 15−16.

(2) Hashim, M. A.; Mukhopadhyay, S.; Sahu, J. N.; Sengupta, B. Remediation Technologies for Heavy Metal Contaminated Groundwater. *J. Environ. Manage.* **2011**, *92*, 2355−2388.

(3) Environmental Protection Agency *Control of Lead and Copper in Drinking Water*; Report no. EPA/625/R-93/001; U.S. Environmental Protection Agency, Office of Research and Development: Cincinnati, OH, 1993.

(4) Rosenzweig, S.; Sorial, G. A.; Sahle-Demessie, E.; Mack, J. Effect of Acid and Alcohol Network Forces within Functionalized Multiwall Carbon Nanotubes Bundles on Adsorption of Copper (II) Species. *Chemosphere* **2013**, *90*, 395−402.

(5) Fu, F.; Wang, Q. Removal of Heavy Metal Ions from Wastewaters: a Review. *J. Environ. Manage.* **2011**, *92*, 407−418.

(6) Qu, X.; Alvarez, P. J. J.; Li, Q. Applications of Nanotechnology in Water and Wastewater Treatment. *Water Res.* **2013**, *47*, 3931−3946.

(7) Khajeh, M.; Laurent, S.; Dastafkan, K. Nanoadsorbents: Classification, Preparation, and Applications (with Emphasis on Aqueous Media). *Chem. Rev.* **2013**, *113*, 7728−7768.

(8) Wu, C. H. Studies of the Equilibrium and Thermodynamics of the Adsorption of Cu(2+) onto As-Produced and Modified Carbon Nanotubes. *J. Colloid Interface Sci.* **2007**, *311*, 338−346.

(9) Wang, J.; Li, Z.; Li, S.; Qi, W.; Liu, P.; Liu, F.; Ye, Y.; Wu, L.; Wang, L.; Wu, W. Adsorption of Cu(II) on Oxidized Multi-Walled Carbon Nanotubes in the Presence of Hydroxylated and Carboxylated Fullerenes. *PLoS One* **2013**, *8*, e72475.

(10) Bayazit, Ş.S.; İnci, İ. Adsorption of Cu (II) Ions from Water by Carbon Nanotubes Oxidized with UV-Light and Ultrasonication. *J. Mol. Liq.* **2014**, *199*, 559−564.

(11) Wang, H.; Ma, H.; Zheng, W.; An, D.; Na, C. Multifunctional and Recollectable Carbon Nanotube Ponytails for Water Purification. *ACS Appl. Mater. Interfaces* **2014**, *6*, 9426−9434.

(12) Dichiara, A. B.; Sherwood, T. J.; Benton-Smith, J.; Wilson, J. C.; Weinstein, S. J.; Rogers, R. E. Free-Standing Carbon Nanotube/Graphene Hybrid Papers as Next Generation Adsorbents. *Nanoscale* **2014**, *6*, 6322−6327.

(13) Dichiara, A. B.; Sherwood, T. J.; Rogers, R. E. Binder Free Graphene-Single-Wall Carbon Nanotube Hybrid Papers for the Removal of Polyaromatic Compounds from Aqueous Systems. *J. Mater. Chem. A* **2013**, *1*, 14480−14483.

(14) Dichiara, A. B.; Benton-Smith, J.; Rogers, R. E. Enhanced Adsorption of Carbon Nanocomposites Exhausted with 2,4-Dichlor-

ophenoxyacetic Acid after Regeneration by Thermal Oxidation and Microwave Irradiation. *Environ. Sci.: Nano* **2014**, *1*, 113−116.

(15) Zhang, C.; Wu, L.; Cai, D.; Zhang, C.; Wang, N.; Zhang, J.; Wu, Z. Adsorption of Polycyclic Aromatic Hydrocarbons (Fluoranthene and Anthracenemethanol) by Functional Graphene Oxide and Removal by pH and Temperature-Sensitive Coagulation. *ACS Appl. Mater. Interfaces* **2013**, *5*, 4783−4790.

(16) Shi, G.; Meng, Q.; Zhao, Z.; Kuan, H. C.; Michelmore, A.; Ma, J. Facile Fabrication of Graphene Membranes with Readily Tunable Structure. *ACS Appl. Mater. Interfaces* **2015**, *7*, 13745.

(17) Li, W.; Dichiara, A.; Bai, J. Carbon Nanotube−Graphene Nanoplatelet Hybrids as High-Performance Multifunctional Reinforcements in Epoxy Composites. *Compos. Sci. Technol.* **2013**, *74*, 221−227.

(18) Khan, U.; O'Connor, I.; Gun'ko, Y. K.; Coleman, J. N. The Preparation of Hybrid Films of Carbon Nanotubes and Nano-Graphite/Graphene with Excellent Mechanical and Electrical Properties. *Carbon* **2010**, *48*, 2825−2830.

(19) Pavese, M.; Musso, S.; Bianco, S.; Giorcelli, M.; Pugno, N. An Analysis of Carbon Nanotube Structure Wettability Before and After Oxidation Treatment. *J. Phys.: Condens. Matter* **2008**, *20*, 474206.

(20) Dresselhaus, M. S.; Jorio, A.; Saito, R. Characterizing Graphene, Graphite, and Carbon Nanotubes by Raman Spectroscopy. *Annu. Rev. Condens. Matter Phys.* **2010**, *1*, 89−108.

(21) Osswald, S.; Havel, M.; Gogotsi, Y. Monitoring Oxidation of Multiwalled Carbon Nanotubes by Raman Spectroscopy. *J. Raman Spectrosc.* **2007**, *38*, 728−736.

(22) Osswald, S.; Flahaut, E.; Gogotsi, Y. In Situ Raman Spectroscopy Study of Oxidation of Double- and Single-Wall Carbon Nanotubes. *Chem. Mater.* **2006**, *18*, 1525−1533.

(23) Kim, U. J.; Furtado, C. A.; Liu, X.; Chen, G.; Eklund, P. C. Raman and IR Spectroscopy of Chemically Processed Single-Walled Carbon Nanotubes. *J. Am. Chem. Soc.* **2005**, *127*, 15437−15445.

(24) Bayazit, Ş.S.; İnci, İ. Adsorption of Pb (II) Ions from Aqueous Solutions by Carbon Nanotubes Oxidized with Different Methods. *J. Ind. Eng. Chem.* **2013**, *19*, 2064−2071.

(25) Balasubramanian, K.; Burghard, M. Chemically Functionalized Carbon Nanotubes. *Small* **2005**, *1*, 180−192.

(26) Park, M.; Kim, B.-H.; Kim, S.; Han, D.-S.; Kim, G.; Lee, K.-R. Improved Binding Between Copper and Carbon Nanotubes in a Composite Using Oxygen-Containing Functional Groups. *Carbon* **2011**, *49*, 811−818.

(27) Lu, C.; Liu, C. Removal of Nickel (II) from Aqueous Solution by Carbon Nanotubes. *J. Chem. Technol. Biotechnol.* **2006**, *81*, 1932−1940.

(28) Glukhova, O.; Slepchenkov, M. Influence of the Curvature of Deformed Graphene Nanoribbons on their Electronic and Adsorptive Properties: Theoretical Investigation Based on the Analysis of the Local Stress Field for an Atomic Grid. *Nanoscale* **2012**, *4*, 3335−3344.

(29) Wang, J.; Chen, Z.; Chen, B. Adsorption of Polycyclic Aromatic Hydrocarbons by Graphene and Graphene Oxide Nanosheets. *Environ. Sci. Technol.* **2014**, *48*, 4817−4825.

(30) Zhu, Y.; Li, L.; Zhang, C.; Casillas, G.; Sun, Z.; Yan, Z.; Ruan, G.; Peng, Z.; Raji, A. R. O.; Kittrell, C.; Hauge, R. H.; Tour, J. M. A Seamless Three-Dimensional Carbon Nanotube Graphene Hybrid Material. *Nat. Commun.* **2012**, *3*, 1225−1228.

(31) Chen, C.; Hu, J.; Shao, D. D.; Li, J. X.; Wang, X. K. Adsorption Behavior of Multiwall Carbon Nanotube/Iron Oxide Magnetic Composites for Ni(II) and Sr(II). *J. Hazard. Mater.* **2009**, *164*, 923−928.

(32) Kadirvelu, K.; Faur-Brasquet, C.; Le Cloirec, P. Removal of Cu(II), Pb(II), and Ni(II) by Adsorption onto Activated Carbon Cloths. *Langmuir* **2000**, *16*, 8404−8409.

(33) Ren, X.; Li, J.; Tan, X.; Wang, X. Comparative Study of Graphene Oxide, Activated Carbon and Carbon Nanotubes as Adsorbents for Copper Decontamination. *Dalton Trans.* **2013**, *42*, 5266−5274.

(34) Li, J.; Chen, C.; Zhang, S.; Wang, X. Surface Functional Groups and Defects on Carbon Nanotubes Affect Adsorption−Desorption

Hysteresis of Metal Cations and Oxoanions in Water. *Environ. Sci.: Nano* **2014**, *1*, 488−495.

(35) Alvarez-Merino, M. A.; Fontecha-Camara, M. A.; Lopez Ramon, M. V.; Moreno-Castilla, C. Temperature Dependence of the Point of Zero Charge of Oxidized and Non-Oxidized Activated Carbons. *Carbon* **2008**, *46*, 778−787.

(36) Borah, D.; Satokawa, S.; Kato, S.; Kojima, T. Characterization of Chemically Modified Carbon Black for Sorption Application. *Appl. Surf. Sci.* **2008**, *254*, 3049−3056.

(37) Borah, D.; Satokawa, S.; Kato, S.; Kojima, T. Sorption of As(V) from Aqueous Solution Using Acid Modified Carbon Black. *J. Hazard. Mater.* **2009**, *162*, 1269−1277.

(38) Zaini, M. A. A.; Okayama, R.; Machida, M. Adsorption of Aqueous Metal Ions on Cattle-Manure-Compost Based Activated Carbons. *J. Hazard. Mater.* **2009**, *170*, 1119−1124.

(39) Sun, W.-L.; Xia, J.; Shan, Y.-C. Comparison Kinetics Studies of Cu(II) Adsorption by Multi-Walled Carbon Nanotubes in Homo and Heterogeneous Systems: Effect of Nano-SiO2. *Chem. Eng. J.* **2014**, *250*, 119−127.

(40) Bystrzejewski, M.; Pyrzynska, K. Kinetics of Copper Ions Sorption onto Activated Carbon, Carbon Nanotubes and Carbon-Encapsulated Magnetic Nanoparticles. *Colloids Surf., A* **2011**, *377*, 402−408.

(41) Langmuir, I. The Constitution and Fundamental Properties of Solids and Liquids. *J. Am. Chem. Soc.* **1916**, *38*, 2221−2295.

(42) Jaroniec, M. Adsorption on Heterogeneous Surfaces: the Exponential Equation for the Overall Adsorption Isotherm. *Surf. Sci.* **1975**, *50*, 553−564.

(43) Wu, C. H. Adsorption of Reactive Dye onto Carbon Nanotubes: Equilibrium, Kinetics and Thermodynamics. *J. Hazard. Mater.* **2007**, *144*, 93−100.

(44) Tofighy, M. A.; Mohammadi, T. Adsorption of Divalent Heavy Metal Ions from Water Using Carbon Nanotube Sheets. *J. Hazard. Mater.* **2011**, *185*, 140−147.

(45) Jiang, T.; Liu, W.; Mao, Y.; Zhang, L.; Cheng, J.; Gong, M.; Zhao, H.; Dai, L.; Zhang, S.; Zhao, Q. Adsorption Behavior of Copper Ions from Aqueous Solution onto Graphene Oxide−CdS Composite. *Chem. Eng. J.* **2015**, *259*, 603−610.

(46) Zhang, Y.; Chi, H.; Zhang, W.; Sun, Y.; Liang, Q.; Gu, Y.; Jing, R. Highly Efficient Adsorption of Copper Ions by a PVP-Reduced Graphene Oxide Based On a New Adsorptions Mechanism. *Nano-Micro Lett.* **2014**, *6*, 80−87.